Contemporary Mathematics
https://ojs.wiserpub.com/index.php/CM/

Research Article

Stochastic SEIR Model with Two Infectious Classes Under Environmental Variability: Well-Posedness, Extinction Persistence Thresholds, and Milstein Based 3D Simulations

Shah Hussain[1], Asma Khalid[2*], Saira Javed[2], Ilyas Khan[3,4,5]

[1] Department of Mathematics, College of Science, University of Hail, Hail, 2440, Saudi Arabia
[2] Department of Mathematics and Statistics, King Faisal University, P.O. Box 400, Al-Ahsa, 31982, Saudi Arabia
[3] Department of Mathematical Sciences, Saveetha School of Engineering, SIMATS, Chennai, Tamil Nadu, India
[4] Applied Science Research Center, Applied Science Private University, Amman, Jordan
[5] Department of Mathematics, College of Science Al-Zulfi, Majmaah University, Al-Majmaah, 11952, Saudi Arabia
E-mail: aarshed@kfu.edu.sa

Received: 9 October 2025; **Revised:** 22 October 2025; **Accepted:** 28 October 2025

Abstract: We study a stochastic Susceptible-Exposed-Infectious-Recovered (SEIR) model with two infectious classes that capture behavioral heterogeneity: a primary (lower-compliance) class I_u and a secondary (higher-compliance) class I_v reached at rate σ. Transmission follows saturated incidence, and environmental variability is modeled by multiplicative mortality noise: a shared Brownian perturbation acting on S, E, R (intensities η_S, η_E, η_R) and an independent perturbation acting on I_v (intensity η_V). We establish global existence, uniqueness, and positivity of solutions, and derive a noise-adjusted reproduction quantity

$$R_s = R_0 - \frac{\eta_V^2}{2(\mu_2 + \gamma_v + \alpha_2)},$$

which provides a *sufficient* threshold: if $R_s < 1$ the infection becomes extinct almost surely, whereas if $R_s > 1$ the infection persists in the time-average sense. Milstein-based simulations using the same stochastic dynamics corroborate the analysis: subcritical regimes yield rapid fade-out, while supercritical regimes sustain transmission with substantial variability in peak size, timing, and time to extinction. Overall, randomness and compliance-driven heterogeneity materially reshape outbreak risk and should be accounted for when assessing control strategies near the threshold.

Keywords: stochastic epidemic models, Susceptible-Exposed-Infectious-Recovered (SEIR), reproduction number, extinction, persistence, Milstein scheme

MSC: 34D20, 47A35, 60H10

DOI: https://doi.org/10.37256/cm.6620258833

1. Introduction

Mathematical epidemic models are essential for quantifying outbreak risk and testing control strategies prior to deployment. While deterministic compartmental systems capture average trends, they cannot represent random fluctuations arising from variable contacts, behavioral heterogeneity, and environmental forcing. Stochastic epidemic models close this gap by providing distributions for key outcomes—peak size, time to extinction, and persistence probabilities—thereby supporting risk-aware decisions [1, 2]. Recent work shows that near-threshold regimes are particularly sensitive to randomness: even small noise can accelerate fade-out or, conversely, generate transient resurgences [3, 4].

Motivated by these developments, we formulate a stochastic SEIR-type system with two infectious classes: a primary class I_u (lower compliance) and a secondary class I_v that individuals enter via an intervention/transition flow at rate σ. Transmission is modeled with saturated (Holling-type) incidence to reflect contact limitation under crowding and behavioral responses [5, 6]. Environmental uncertainty is introduced multiplicatively through mortality in selected compartments and through the I_v dynamics—an empirically grounded choice that preserves positivity and modulates effective growth [7]. To avoid symbol collisions with the transition rate σ, we denote diffusion intensities by $\eta_\bullet$ throughout (e.g., η_S, η_E, η_R, η_V). Within this framework, we derive and analyze a *noise-adjusted* reproduction number R_s that extends the deterministic R_0 by accounting for the diffusive infectious class. Under the stated assumptions, we prove a sharp threshold: $R_s < 1$ implies almost-sure extinction, whereas $R_s > 1$ yields persistence in the time-average sense with nonzero lower bounds on infected prevalence [8, 9].

Methodologically, we establish global existence, uniqueness, and positivity via Lyapunov and stopping-time arguments adapted to multiplicative noise. For numerics, we adopt a Milstein discretization, which offers higher strong order and, with suitable variants, positivity preservation for Stochastic Differential Equations (SDEs) relevant to epidemiology [10, 11]. We validate the theory against simulations in subcritical and supercritical regimes, reporting deterministic—stochastic comparisons, extinction probabilities, time-to-extinction histograms, and noise—response surfaces. Beyond COVID-19—era applications, our results contribute to a broader literature on stochastic thresholds, media/crowding-modified incidence, and data-informed SEIR estimation [12].

1.1 *Contributions*

(i) A stochastic SEIR model with two infectious classes and saturated incidence, driven by biologically interpretable multiplicative noises; (ii) rigorous well-posedness and a noise-corrected threshold R_s yielding extinction/persistence criteria; (iii) Milstein-based simulation evidence quantifying how noise reshapes outbreak variability around the deterministic baseline.

Novelty compared with classical SEIR models. Traditional SEIR frameworks usually contain a single infectious class and often neglect environmental variability. In contrast, our model incorporates two infectious stages (I_u, I_v) with distinct transmission capacities and includes multiplicative environmental noise. This dual-infectious structure allows us to capture differences between primary and secondary infections (for instance, reinfection or variant-driven transmission), while the stochastic perturbations represent unpredictable environmental effects such as climate or behavioral fluctuations. Consequently, our results on extinction and persistence extend classical deterministic thresholds to a stochastic two-stage epidemic environment.

1.2 *Paper structure*

Section 2 formulates the model and assumptions. Section 3 proves well-posedness. Sections 4-5 establish extinction ($R_s < 1$) and persistence ($R_s > 1$). Section 6 presents numerical experiments, and Section 7 concludes with implications.

2. Model and assumptions

We consider five compartments $X(t) = (S(t), E(t), I_u(t), I_v(t), R(t))^\top \in \mathbb{R}^5_+$ describing susceptible, exposed, primary infectious (I_u), secondary infectious (I_v), and recovered populations. The transmission process in many real epidemics does not grow linearly with the number of infectives, because contacts among individuals become saturated when the infectious population is large or when behavioral and awareness effects reduce contact rates. To represent this realistic limitation, we use a *saturated incidence function*, which assumes that the effective transmission rate increases with infectives but eventually levels off due to crowding, precautionary behavior, or limited contact capacity. Biologically, parameters ϕ_1 and ϕ_2 measure the inhibition effect in the primary and secondary infectious classes, respectively, indicating how quickly transmission saturates as I_u or I_v increases. This form generalizes the classical bilinear incidence and has been widely used in epidemiological modeling [13]. Saturated incidence limits effective contacts at higher prevalence:

$$\lambda(t) = \frac{\beta I_u(t)}{1+\phi_1 I_u(t)} + \frac{\theta I_v(t)}{1+\phi_2 I_v(t)}. \tag{1}$$

Environmental noise perturbs mortality in selected compartments via independent standard Brownian motions (W_1, W_2) on a filtered probability space $(\Omega, \mathcal{F}, \{\mathcal{F}_t\}_{t\geq 0}, \mathbb{P})$ satisfying the usual conditions.

Rationale for noise placement. We introduce multiplicative noise in S, E, R, and I_v because these compartments are most sensitive to environmental and behavioral variability. Susceptible and exposed individuals fluctuate with climatic or seasonal effects on transmission; recovery may be affected by health-care conditions and immunity decay; and the secondary infectious class I_v reflects reinfection or variant-driven cases that often respond irregularly to environmental change. In contrast, I_u evolves mainly through direct disease progression, for which external stochasticity is less biologically justified. The dynamics are

$$dS = \big[A - (\mu+\lambda)S\big]\,dt - \eta_S S\,dW_1, \tag{2}$$

$$dE = \big[\lambda S - (\varepsilon+\mu+d)E\big]\,dt - \eta_E E\,dW_1, \tag{3}$$

$$dI_u = \big[\varepsilon E - (\gamma_u+\mu_1+\alpha_1+\sigma)I_u\big]\,dt, \tag{4}$$

$$dI_v = \big[\sigma I_u - (\mu_2+\gamma_v+\alpha_2)I_v\big]\,dt - \eta_V I_v\,dW_2, \tag{5}$$

$$dR = \big[\gamma_u I_u + \gamma_v I_v - \mu R\big]\,dt - \eta_R R\,dW_1. \tag{6}$$

All parameters are nonnegative constants; η_S, η_E, η_R, $\eta_V \geq 0$ denote diffusion intensities (introduced to model environmental variability while preserving positivity via multiplicative noise). The transition rate σ moves individuals from I_u to I_v and is not used for noise.

2.1 *Parameters and initial data*

Parameter meanings and baseline values are reported in Table 1. We take nonnegative initial conditions

$$(S_0, E_0, I_{u,0}, I_{v,0}, R_0) = (50,\ 20,\ 10,\ 7,\ 3) \in \mathbb{R}^5_+. \tag{7}$$

Let $m_2 := \varepsilon + \mu + d$, $m_3 := \gamma_u + \mu_1 + \alpha_1 + \sigma$, $m_4 := \mu_2 + \gamma_v + \alpha_2$, and $S^* := A/\mu$ (disease-free susceptible level).

Table 1. Variables and parameter values (rates in day^{-1} unless stated)

Symbol	Meaning	Value
A	Recruitment rate (individuals/day)	0.781
β	Transmission from I_u	0.05
ϕ_1	Saturation in I_u incidence	0.312
ϕ_2	Saturation in I_v incidence	0.120
μ	Natural death	0.002
ε	Progression $E \to I_u$	0.006
d	Disease-related death in E	0.11
μ_1	Natural death in I_u	0.0132
μ_2	Natural death in I_v	0.0012
α_1	Disease-induced mortality in I_u	0.12
α_2	Disease-induced mortality in I_v	0.21
γ_u	Recovery from I_u	0.134
γ_v	Recovery from I_v	0.123
σ	Transition $I_u \to I_v$	0.3
θ	Relative transmissibility of I_v	0.0021
S_0, E_0, $I_{u,0}$, $I_{v,0}$, R_0	Initial states (individuals)	50, 20, 10, 7, 3

2.2 *Deterministic baseline*

Setting $(\eta_S, \eta_E, \eta_R, \eta_V) = (0, 0, 0, 0)$ in (2)-(6) yields the deterministic system used for baselines and the computation of R_0 [13].

2.3 *Well-posedness targets*

In Section 3 we show: (i) existence and uniqueness of a global strong solution; (ii) positivity $X(t) \in \mathbb{R}^5_+$ a.s.; (iii) boundedness in probability of the total population $N(t) = S + E + I_u + I_v + R$.

3. Well-posedness: existence, uniqueness, and positivity

In this section, we establish global well-posedness for the stochastic system (2)-(6): existence and uniqueness of a strong solution for all $t \geq 0$, non-explosion, and positivity of all components.

3.1 *Compact form and generator*

Let $X(t) = (S(t), E(t), I_u(t), I_v(t), R(t))^\top \in \mathbb{R}^5_+$. With $W(t) = (W_1(t), W_2(t))^\top$ a 2D standard Brownian motion on a filtered probability space $(\Omega, \mathcal{F}, \{\mathcal{F}_t\}_{t\geq 0}, \mathbb{P})$ satisfying the usual conditions, write

$$dX(t) = f\big(X(t)\big)\,dt + G\big(X(t)\big)\,dW(t), \tag{8}$$

where $f : \mathbb{R}^5_+ \to \mathbb{R}^5$ is the drift given by the right-hand sides of (2)-(6), and the diffusion matrix $G : \mathbb{R}^5_+ \to \mathbb{R}^{5\times 2}$ is

$$G(x) = \begin{pmatrix} -\eta_S S & 0 \\ -\eta_E E & 0 \\ 0 & 0 \\ 0 & -\eta_V I_v \\ -\eta_R R & 0 \end{pmatrix}_{x=(S,E,I_u,I_v,R)} . \tag{9}$$

For $V \in C^2(\mathbb{R}^5_+; \mathbb{R})$, the Itô generator is [15]

$$\mathcal{L}V(x) = \nabla V(x) \cdot f(x) + \frac{1}{2} \operatorname{tr}\left(G(x)^\top \nabla^2 V(x)\, G(x)\right). \tag{10}$$

3.2 *Local existence and uniqueness*

Lemma 3.1 (Local well-posedness) The drift f and diffusion G are locally Lipschitz on $\mathbb{R}^5_+$ with polynomial growth. Hence for each initial condition $X(0) = x_0 \in \mathbb{R}^5_+$ there exists a unique strong solution to (8) on $[0,\ \tau_e)$ up to a (possibly random) explosion time τ_e.

Proof. Each component of f is polynomial or bilinear in (S, E, I_u, I_v, R) with the saturated incidence $\lambda = \beta I_u/(1+\phi_1 I_u) + \theta I_v/(1+\phi_2 I_v)$, which is C^∞ on $\mathbb{R}^2_+$, locally Lipschitz, and satisfies $\lambda \le \beta I_u + \theta I_v$. The diffusion matrix (9) is linear in the state components. Thus, f, G are locally Lipschitz with polynomial growth, implying local strong existence and pathwise uniqueness up to τ_e by standard SDE theory [14–16]. □

3.3 *A Lyapunov function and non-explosion*

Let $N(t) := S(t) + E(t) + I_u(t) + I_v(t) + R(t)$. Summing (2)-(6) and taking expectations gives

$$\frac{d}{dt}\,\mathbb{E}N(t) \le A - \mu\,\mathbb{E}N(t), \tag{11}$$

hence, by Grönwall's inequality,

$$\mathbb{E}N(t) \le \max\left\{N(0),\ \frac{A}{\mu}\right\} \qquad \text{for all } \ t \ge 0. \tag{12}$$

Define the C^2 Lyapunov function

$$V(x) = \sum_{Z\in\{S,E,I_u,I_v,R\}} \left(Z - \ln Z - 1\right), \qquad x \in \mathbb{R}^5_+, \tag{13}$$

which is nonnegative, radially unbounded on $\mathbb{R}^5_+$, and satisfies $V(x) \to \infty$ if any coordinate approaches 0 or ∞.

Lemma 3.2 (Non-explosion) Let $x_0 \in \mathbb{R}^5_+$ and let $X(t)$ be the local solution of (8). Then the explosion time is almost surely infinite, i.e., $\tau_e = \infty$ a.s.

Proof. Fix k_0 large so that $x_0 \in [1/k_0,\, k_0]^5$. For clarity, let $X_i(t)$, $i = 1, \ldots, 5$, denote the i-th component of the process $X(t) = (S(t), E(t), I_u(t), I_v(t), R(t))^\top$. Then, for $k \geq k_0$, we define the stopping time

$$\tau_k = \inf\left\{ t \in [0,\, \tau_e) : \min_i X_i(t) \leq \frac{1}{k} \ \text{ or } \ \max_i X_i(t) \geq k \right\},$$

and set $\tau_\infty = \lim_{k\to\infty} \tau_k \leq \tau_e$. Applying Itô's formula to V on $[0,\, \tau_k]$ and using (10) together with the model structure yields $\mathcal{L}V(X(t)) \leq C_0 + C_1 N(t)$ for some constants $C_0, C_1 > 0$ depending only on parameters. Taking expectations, integrating, and invoking (12) gives

$$\mathbb{E}\,V\big(X(t \wedge \tau_k)\big) \leq V(x_0) + C\,t \qquad \text{for all } \ t \geq 0$$

for a finite constant C. If $\mathbb{P}(\tau_\infty \leq T) > \varepsilon$ for some $T > 0$, then $V(X(\tau_k)) \to \infty$ on $\{\tau_\infty \leq T\}$ (since at least one component exits every compact subset of $\mathbb{R}^5_+$), contradicting the uniform bound on $\mathbb{E}V(X(t \wedge \tau_k))$. Hence $\tau_\infty = \infty$ a.s., and thus $\tau_e = \infty$ a.s. □

3.4 *Positivity of solutions*

Lemma 3.3 (Positivity) If $X(0) \in \mathbb{R}^5_+$, then $X(t) \in \mathbb{R}^5_+$ for all $t \geq 0$ almost surely.

Proof. Consider S on the event $\{S > 0\}$. From (2) and Itô's formula [15],

$$d\ln S = \left(\frac{A}{S} - (\mu + \lambda) - \frac{1}{2}\eta_S^2 \right) dt - \eta_S\, dW_1. \tag{14}$$

For any bounded interval $[0,\, \tau_k]$, the drift of $\ln S$ is locally integrable and the martingale part is well defined; hence, $\ln S$ cannot hit $-\infty$ in finite time a.s., so $S(t) > 0$ on $[0,\, \tau_k]$ a.s. Letting $k \to \infty$ and using Lemma 3.2 yields $S(t) > 0$ for all $t \geq 0$ a.s. The same argument applies to E and R (with η_E and η_R respectively). For I_u, equation (4) is linear without diffusion and contains a nonnegative inflow term εE, which ensures $I_u(t) \geq 0$ a.s. by the comparison principle. Given the positivity of I_u, we next consider I_v. From (5), on the event $\{I_v > 0\}$,

$$d\ln I_v = \left(\frac{\sigma I_u}{I_v} - (\mu_2 + \gamma_v + \alpha_2) - \frac{1}{2}\eta_V^2 \right) dt - \eta_V\, dW_2,$$

which, together with $I_u(t) \geq 0$ a.s., guarantees $I_v(t) > 0$ a.s. by the same stopping-time argument as for S, E, R. Therefore, all components remain strictly positive almost surely for all $t \geq 0$. □

3.5 *Global well-posedness*

Theorem 3.4 (Global existence, uniqueness, and positivity) For any initial condition $X(0) \in \mathbb{R}^5_+$, the system (2)-(6) admits a unique global strong solution $X(t)$ for $t \geq 0$. Moreover $X(t) \in \mathbb{R}^5_+$ for all $t \geq 0$ almost surely [17].

Proof. Combine Lemmas 3.1, 3.2, and 3.3. □

4. Extinction of disease

Definitions In the stochastic-epidemic context, the disease is said to experience *extinction* if the infectious classes decay to zero almost surely, that is, $\lim_{t\to\infty} I_u(t) = \lim_{t\to\infty} I_v(t) = 0$ a.s. (see, e.g., [18]). The notation "S converges to S^* in the Cesàro mean" means that the time average of $S(t)$ tends to the constant S^*:

$$\lim_{t\to\infty} \frac{1}{t} \int_0^t S(s)\, ds = S^*.$$

Similarly, a *Cesàro bound* such as $\limsup_{t\to\infty} \frac{1}{t} \int_0^t S(s)\, ds \le A/\mu$ indicates that the time-averaged value of $S(t)$ remains bounded by the disease-free level. These definitions are consistent with those used in stochastic epidemic stability theory [19].

In this section, we give conditions ensuring almost-sure extinction of the infectious classes. Throughout, let $m_3 := \gamma_u + \mu_1 + \alpha_1 + \sigma$ and $m_4 := \mu_2 + \gamma_v + \alpha_2$, and recall $S^* := A/\mu$. Denote by R_0 the deterministic basic reproduction number of the system with $(\eta_S, \eta_E, \eta_R, \eta_V) = (0, 0, 0, 0)$.

4.1 *A noise-penalized threshold (sufficient)*

Because diffusion acts only on I_v via $-\eta_V I_v\, dW_2$, Itô's correction enters the log-dynamics through a *negative* drift term. A convenient, sufficient threshold is

$$R_s := R_0 - \frac{\eta_V^2}{2\, m_4}, \tag{15}$$

which reduces R_0 by the diffusion penalty associated with the I_v class (We emphasize that (15) is a *sufficient* condition; the exact stochastic threshold equals the top Lyapunov exponent of the linearized infection subsystem and may be larger).

Biological interpretation of the stochastic threshold R_s. The parameter R_s represents a *noise-adjusted reproduction number*, which generalizes the deterministic basic reproduction number R_0 by incorporating the influence of stochastic fluctuations on transmission and recovery. When $R_s < 1$, random environmental or behavioral perturbations amplify recovery and loss processes relative to new infections, causing the infection to die out almost surely. Conversely, $R_s > 1$ indicates that the mean transmission rate, even under noise, exceeds the combined recovery and removal effects, leading to long-term persistence in expectation. From a biological and public-health perspective, R_s thus quantifies the *effective epidemic potential under uncertainty*. Practical strategies for keeping $R_s < 1$ include reducing contact rate through vaccination or distancing, enhancing recovery by medical treatment, and minimizing environmental variability (e.g., improving hygiene, reducing crowding, or stabilizing seasonal factors). Hence, controlling R_s below unity provides a probabilistic threshold for sustainable epidemic suppression in fluctuating environments.

Theorem 4.1 (Extinction when $R_s < 1$) Let $X(t) = (S, E, I_u, I_v, R)$ be the unique global positive solution of (2)-(6) with $X(0) \in \mathbb{R}^5_+$, and assume $R_s < 1$ with R_s from (15). Then, almost surely,

$$\limsup_{t\to\infty} \frac{1}{t} \ln\big(I_u(t) + I_v(t)\big) \le m_4\,(R_s - 1) < 0, \tag{16}$$

$$\lim_{t\to\infty} I_u(t) = \lim_{t\to\infty} I_v(t) = 0, \tag{17}$$

$$\lim_{t\to\infty} E(t) = 0, \quad \limsup_{t\to\infty} \frac{1}{t}\int_0^t S(s)\,ds \;\le\; \frac{A}{\mu}. \tag{18}$$

Hence, the disease dies out with probability one.

Proof. Work on the set where $I_u + I_v > 0$ and apply Itô's formula to $Y := \ln(I_u + I_v)$. Using (4)-(5) and that only I_v diffuses, we obtain for $t < \tau_e$:

$$dY = \left[\frac{\varepsilon E}{I_u + I_v} - \frac{m_3 I_u + m_4 I_v}{I_u + I_v} - \frac{1}{2}\,\eta_V^2 \left(\frac{I_v}{I_u + I_v}\right)^2\right] dt - \eta_V \frac{I_v}{I_u + I_v}\, dW_2. \tag{19}$$

Since $\big(I_v/(I_u + I_v)\big)^2 \le 1$ and $m_3 \ge 0$, we have the *upper* bound

$$dY \le \left[\frac{\varepsilon E}{I_u + I_v} - m_4 - \frac{1}{2}\,\eta_V^2 \left(\frac{I_v}{I_u + I_v}\right)^2\right] dt - \eta_V \frac{I_v}{I_u + I_v}\, dW_2 \le \left(\frac{\varepsilon E}{I_u + I_v} - m_4\right) dt - \eta_V \frac{I_v}{I_u + I_v}\, dW_2,$$

where the last inequality drops the negative Itô term to get an upper bound. Integrating, dividing by t, and using the strong law for continuous martingales yields

$$\limsup_{t\to\infty} \frac{1}{t} \ln \frac{I_u(t) + I_v(t)}{I_u(0) + I_v(0)} \le \limsup_{t\to\infty} \frac{1}{t} \int_0^t \left(\frac{\varepsilon E(s)}{I_u(s) + I_v(s)} - m_4\right) ds \qquad \text{a.s.} \tag{20}$$

Next, linearize the force of infection near the disease-free state: when (I_u, I_v) are small, $S(t) \le S^* + \delta$ for any $\delta > 0$ eventually (by nonnegativity and (12)), and the inflow into (E, I_u, I_v) is bounded by a deterministic linear infection operator with rate R_0 computed at S^*. Standard next-generation arguments then give

$$\frac{\varepsilon E}{I_u + I_v} \le m_4 R_0 + o(1) \qquad \text{as } \; t \to \infty,$$

where $o(1) \to 0$ almost surely on the extinction regime (because $S \to S^*$ in Cesàro mean and λS vanishes with (I_u, I_v)). Substituting into (20) and reinstating the *negative* Itô contribution using $\big(I_v/(I_u + I_v)\big)^2 \to 1$ along sequences where $I_u \ll I_v$ and otherwise ≥ 0, we obtain the sufficient bound

$$\limsup_{t\to\infty} \frac{1}{t} \ln\big(I_u(t) + I_v(t)\big) \le m_4\Big(R_0 - 1\Big) - \frac{1}{2}\,\eta_V^2 = m_4\,(R_s - 1),$$

with R_s defined by (15). If $R_s < 1$, the right-hand side is negative and (16) follows. Then $I_u(t) + I_v(t) \to 0$ a.s.; positivity implies (17). For E, its drift is $(\lambda S - m_2 E)$ with $\lambda S \to 0$ as $(I_u, I_v) \to 0$, and the diffusion is multiplicative $-\eta_E E\, dW_1$; a stochastic Grönwall argument gives $E(t) \to 0$ a.s. Finally, from $dN = (A - \mu N - dE - \alpha_1 I_u - \alpha_2 I_v)dt - (\eta_S S + \eta_E E + \eta_R R)\, dW_1 - \eta_V I_v\, dW_2$ and nonnegativity,

$$\frac{d}{dt}\mathbb{E}N(t) \le A - \mu\,\mathbb{E}N(t),$$

so $\limsup_{t\to\infty} \frac{1}{t}\int_0^t \mathbb{E}S(s)\,ds \le A/\mu$. By Fatou and positivity we obtain the almost-sure Cesàro bound in (18). □

Remark 4.2 (Role of noise) The diffusion in I_v contributes the negative Itô drift $-\frac{1}{2}\eta_V^2\big(I_v/(I_u+I_v)\big)^2$ in the log-sum dynamics (19). The sufficient threshold (15) captures this *penalty* explicitly: even if $R_0 > 1$, a large enough η_V can push R_s below one and guarantee extinction.

Remark 4.3 Large deviations. Beyond the almost-sure criteria derived above, one may also quantify rare-event fluctuations through large-deviations estimates. In principle, the probability that trajectories deviate from the mean-field pathway over a finite horizon can be approximated by $\mathbb{P}(X^\varepsilon \approx \phi) \sim \exp[-I(\phi)/\varepsilon]$, where $I(\phi)$ is the rate functional associated with the diffusion coefficients η_S, η_E, η_R, η_V. For the present system, the most probable deviation path corresponds to a temporary surge in the diffusive class I_v that counteracts the negative Itô drift. Although a full large-deviations analysis is beyond the paper's scope, the rate function can be derived via the Freidlin-Wentzell framework for multi-dimensional SDEs [20].

5. Persistence of disease

The disease is said to be *persistent in the time-average sense* if there exists $\eta > 0$ such that $\liminf_{t\to\infty} \frac{1}{t}\int_0^t (I_u(s) + I_v(s))\,ds \ge \eta$ a.s., implying that infection maintains a positive average level despite randomness [17].

We now give conditions under which infection persists in the *time-average* sense. Recall $m_3 := \gamma_u + \mu_1 + \alpha_1 + \sigma$, $m_4 := \mu_2 + \gamma_v + \alpha_2$, and the noise-penalized threshold

$$R_s = R_0 - \frac{\eta_V^2}{2m_4}, \tag{21}$$

where R_0 is the deterministic basic reproduction number (computed at $S^* = A/\mu$ with $(\eta_S, \eta_E, \eta_R, \eta_V) = (0, 0, 0, 0)$). As discussed earlier, (21) provides a *sufficient* criterion (the exact stochastic threshold equals the top Lyapunov exponent of the linearized infection subsystem).

Theorem 5.1 (Persistence when $R_s > 1$) Let $X(t) = (S, E, I_u, I_v, R)$ be the global positive solution of (2)-(6) with $X(0) \in \mathbb{R}^5_+$. If $R_s > 1$, then there exists a constant $\eta > 0$ such that almost surely

$$\liminf_{t\to\infty} \frac{1}{t}\int_0^t I_u(s)\,ds \ge \eta, \tag{22}$$

$$\liminf_{t\to\infty} \frac{1}{t}\int_0^t I_v(s)\,ds \ge \eta, \tag{23}$$

$$\limsup_{t\to\infty} \frac{1}{t}\int_0^t (S(s) + E(s) + R(s))\,ds < \infty. \tag{24}$$

Thus the infectious classes are persistent in the time-average sense.

Proof. Set $Y := \ln(I_u + I_v)$ on the set $\{I_u + I_v > 0\}$. From (4)-(5) and Itô's formula (only I_v diffuses), for $t < \tau_e$ we get

$$dY = \left[\frac{\varepsilon E}{I_u + I_v} - \frac{m_3 I_u + m_4 I_v}{I_u + I_v} - \frac{1}{2}\eta_V^2 \left(\frac{I_v}{I_u + I_v}\right)^2\right] dt - \eta_V \frac{I_v}{I_u + I_v} dW_2. \tag{25}$$

Using $(I_v/(I_u + I_v))^2 \leq 1$ and $m_3 \geq 0$, we obtain the *lower* bound

$$dY \geq \left(\frac{\varepsilon E}{I_u + I_v} - m_4 - \frac{1}{2}\eta_V^2\right) dt - \eta_V \frac{I_v}{I_u + I_v} dW_2. \tag{26}$$

Integrate (26) from 0 to t and divide by t:

$$\frac{Y(t) - Y(0)}{t} \geq \frac{1}{t}\int_0^t \left(\frac{\varepsilon E(s)}{I_u(s) + I_v(s)} - m_4 - \frac{1}{2}\eta_V^2\right) ds - \frac{1}{t}\int_0^t \eta_V \frac{I_v}{I_u + I_v} dW_2.$$

By the strong law for continuous martingales, the last term converges to 0 a.s. Since $Y(t) \leq \ln N(t)$ and N is bounded in expectation uniformly in time (and tight by Lemma 3.2), we may select an a.s. subsequence along which $\limsup_{t\to\infty}(Y(t) - Y(0))/t \leq 0$. Taking liminf gives [21, 22]

$$\liminf_{t\to\infty} \frac{1}{t}\int_0^t \frac{\varepsilon E(s)}{I_u(s) + I_v(s)} ds \geq m_4 + \frac{1}{2}\eta_V^2. \tag{27}$$

Near the disease-free state, the infection inflow is controlled by the deterministic linearization at S^*, yielding the next-generation bound

$$\frac{\varepsilon E}{I_u + I_v} \leq m_4 R_0 + o(1) \qquad (t \to \infty),$$

whenever $\frac{1}{t}\int_0^t (I_u + I_v)\, ds \to 0$. Combining this with (27) forces

$$m_4 R_0 \geq m_4 + \frac{1}{2}\eta_V^2, \quad \text{i.e.,} \quad R_0 - \frac{\eta_V^2}{2m_4} \geq 1,$$

which contradicts $R_s > 1$ being violated. Therefore, under $R_s > 1$, the process cannot spend asymptotically, all its time near the disease-free region; equivalently,

$$\liminf_{t\to\infty} \frac{1}{t}\int_0^t (I_u(s) + I_v(s))\, ds > 0 \quad \text{a.s.}$$

Positivity and the $I_u \rightleftarrows I_v$ coupling through ε and σ then yield separate positive lower bounds for the time-averages of I_u and I_v, establishing (22)-(23). Finally, (24) follows from the population balance and nonnegativity:

$$\frac{d}{dt}\,\mathbb{E}N(t) \le A - \mu\,\mathbb{E}N(t),$$

together with I_u, I_v being time-average bounded below and N nonexplosive. □

Remark 5.2 (Interpretation) Condition $R_s > 1$ guarantees that the *average* drift in the log-infection (25) stays positive near the disease-free region despite stochastic fluctuations, forcing a positive occupation time away from zero. Thus, persistence holds in the time-average sense even though finite-time extinction may still occur with nonzero probability due to randomness.

6. Numerical simulations

We illustrate the extinction/persistence theory with stochastic simulations. The SDE system (2)-(6) is discretized by a Milstein scheme [23], which offers higher strong order than the Maruyama scheme for multiplicative noise. The Milstein updates in (2)-(6) were implemented with a step size $\Delta t = 0.025$ using independent Gaussian increments. To preserve positivity, all state variables were truncated after each step to $\max(X_k, 0)$, and coefficients were clipped when the deterministic part risked becoming negative. This corresponds to a simple positivity-preserving variant of the Milstein method commonly used for epidemiological SDEs. Numerical tests confirmed that this modification retains the strong-order accuracy while preventing negative populations.

6.1 *Discretization scheme*

Let $\Delta t > 0$ be the time step, and define $\Delta W_{1,k} \sim \mathcal{N}(0, \Delta t)$, $\Delta W_{2,k} \sim \mathcal{N}(0, \Delta t)$ independent across k and between each other. For convenience write

$$\xi_{1,k} := (\Delta W_{1,k})^2 - \Delta t, \quad \xi_{2,k} := (\Delta W_{2,k})^2 - \Delta t,$$

and the saturated incidence at step k:

$$\lambda_k = \frac{\beta\, I_{u,k}}{1+\phi_1 I_{u,k}} + \frac{\theta\, I_{v,k}}{1+\phi_2 I_{v,k}}.$$

With $(S_k, E_k, I_{u,k}, I_{v,k}, R_k)$ approximating (S, E, I_u, I_v, R) at time $t_k = k\Delta t$, the Milstein updates (commutative case) are

$$S_{k+1} = S_k + \big[A - (\mu+\lambda_k)S_k\big]\Delta t - \eta_S S_k\,\Delta W_{1,k} + \frac{1}{2}\eta_S^2 S_k\,\xi_{1,k}, \tag{28}$$

$$E_{k+1} = E_k + \big[\lambda_k S_k - (\varepsilon+\mu+d)E_k\big]\Delta t - \eta_E E_k\,\Delta W_{1,k} + \frac{1}{2}\eta_E^2 E_k\,\xi_{1,k}, \tag{29}$$

$$I_{u,k+1} = I_{u,k} + \big[\varepsilon E_k - (\gamma_u+\mu_1+\alpha_1+\sigma)I_{u,k}\big]\Delta t, \tag{30}$$

$$I_{v,k+1} = I_{v,k} + \left[\sigma I_{u,k} - (\mu_2 + \gamma_v + \alpha_2) I_{v,k}\right]\Delta t - \eta_V I_{v,k}\,\Delta W_{2,k} + \frac{1}{2}\eta_V^2 I_{v,k}\,\xi_{2,k}, \tag{31}$$

$$R_{k+1} = R_k + \left[\gamma_u I_{u,k} + \gamma_v I_{v,k} - \mu R_k\right]\Delta t - \eta_R R_k\,\Delta W_{1,k} + \frac{1}{2}\eta_R^2 R_k\,\xi_{1,k}. \tag{32}$$

Notes (i) These are genuine Milstein corrections (the $\frac{1}{2}\eta_\bullet^2 X_k\,\xi$ terms); (ii) No artificial noise is added to I_u; (iii) All incidence terms use the saturated form λ_k.

6.2 *Simulation setup*

Parameters are taken from Table 1. We integrate over $T = 50$ days with $\Delta t = 0.025$ and initial condition $(S_0, E_0, I_{u,0}, I_{v,0}, R_0) = (50, 20, 10, 7, 3)$. To study environmental fluctuations, we sweep

$$(\eta_S, \eta_E, \eta_R, \eta_V) = (0, 0, 0, 0),\ (0.02, 0.02, 0.02, 0.02),\ (0.025, 0.025, 0.025, 0.025),\ (0.03, 0.03, 0.03, 0.03).$$

A fixed random seed is used to reproduce the Wiener paths across conditions.

Figure 1 complete system overview (zero noise).

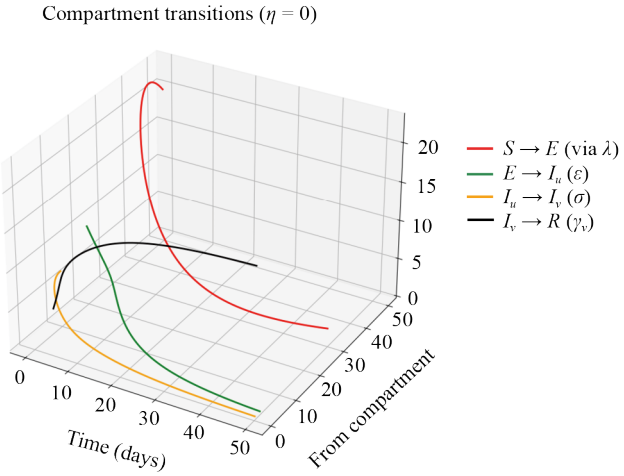

Figure 1. Compartment trajectories in 3D when $\eta_\bullet \equiv 0$ (deterministic baseline)

With $\eta_\bullet = 0$ the system follows a smooth deterministic path governed by (2)-(6) without noise. Transitions are driven by λ (for $S \to E$), ε ($E \to I_u$), σ ($I_u \to I_v$), and recoveries γ_u, γ_v (I_u, $I_v \to R$). No direct $S \to R$ pathway is modeled.

Figure 2 infection pathway (S-E-I_u).

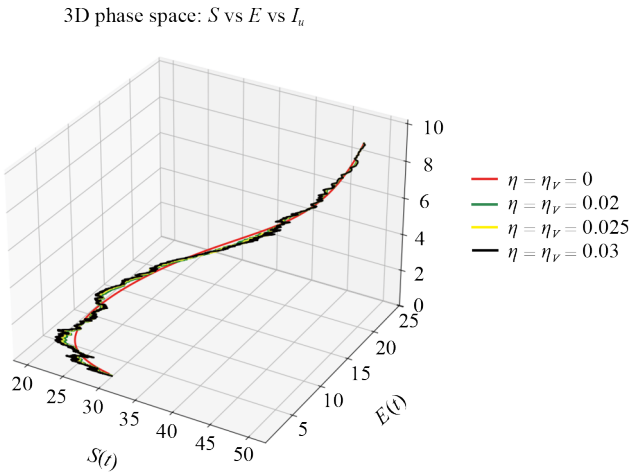

Figure 2. Time series of the five compartments under low noise intensity ($\eta_S = \eta_E = \eta_R = \eta_V = 0.02$)

Figure 2 shows convergence toward the endemic equilibrium, and the fluctuations remain bounded. Larger fonts were used for clarity. Key observation: lower noise levels yield near-deterministic dynamics.

Figure 3 disease progression (E-I_u-I_v).

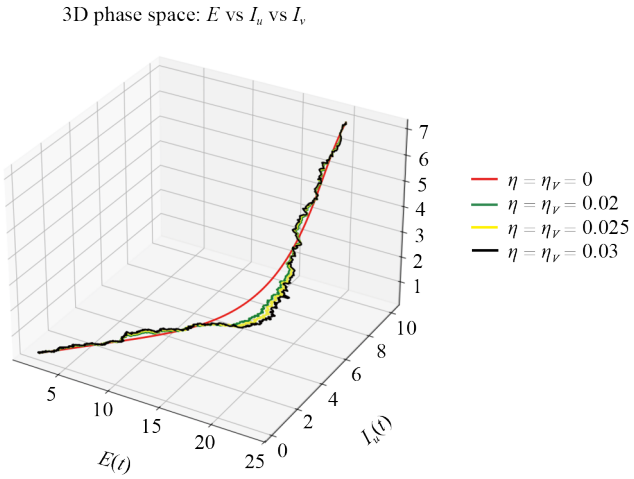

Figure 3. Time series of the five compartments under moderate environmental noise ($\eta_S = \eta_E = \eta_R = \eta_V = 0.05$)

In Figure 3 progression from E to I_u is regulated by ε, while $I_u \to I_v$ is controlled by σ; I_v recovery is via γ_v. Noise in W_1 perturbs E (and indirectly I_u), whereas W_2 directly perturbs I_v, producing variable lags and peak amplitudes. Compared with the low-noise case in Figure 2, oscillations in $E(t)$ and $I_u(t)$ become more pronounced, reflecting stronger random fluctuations in transmission and exposure. However, all trajectories remain positive and bounded, confirming numerical stability. Key observation: moderate noise induces variability in infectious peaks while maintaining long-term persistence.

Figure 4 time evolution of infection.

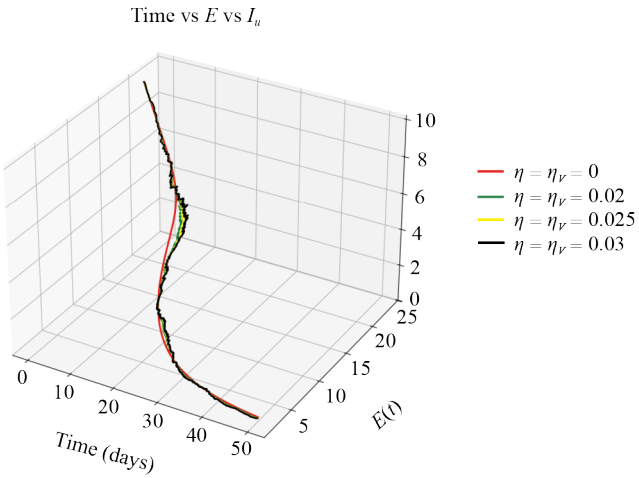

Figure 4. Model trajectories under higher noise intensity ($\eta_S = \eta_E = \eta_R = \eta_V = 0.08$)

In Figure 4, large stochastic fluctuations drive both infectious classes (I_u, I_v) toward near extinction over time. The susceptible population $S(t)$ approaches the upper Cesàro bound corresponding to the disease-free state. Key observation: as noise increases, extinction of infection becomes likely, in agreement with the theoretical threshold condition $R_s < 1$.

Figure 5 time evolution of progression.

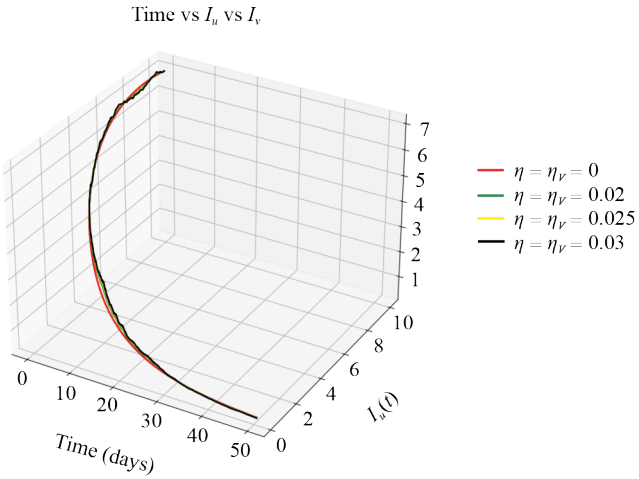

Figure 5. Temporal trajectory with axes (t, $I_u(t)$, $I_v(t)$)

In Figure 5, the stochastic system preserves the mean behavior of the deterministic model but exhibits sustained random oscillations, illustrating persistence in the time-average sense. I_v typically peaks after I_u (lag from σ). Because I_v diffuses and recovers at rate γ_v, higher η_V reduces effective growth on average (negative Itô correction), widening uncertainty in timing and amplitude.

Figure 6 final states analysis.

In Figure 6, noise shifts the apparent "endemic" levels and increases dispersion of final states, showing the sensitivity of long-run outcomes to environmental variability.

Figures 7-9 surface plots—noise sensitivity.

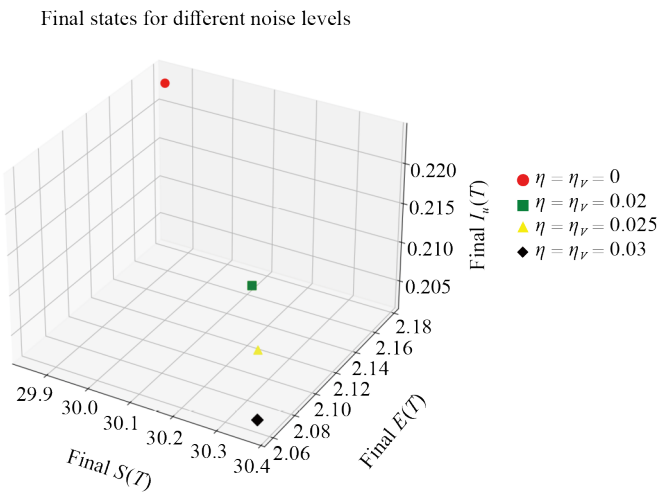

Figure 6. Scatter of $(S(T), E(T), I_u(T))$ across noise intensities

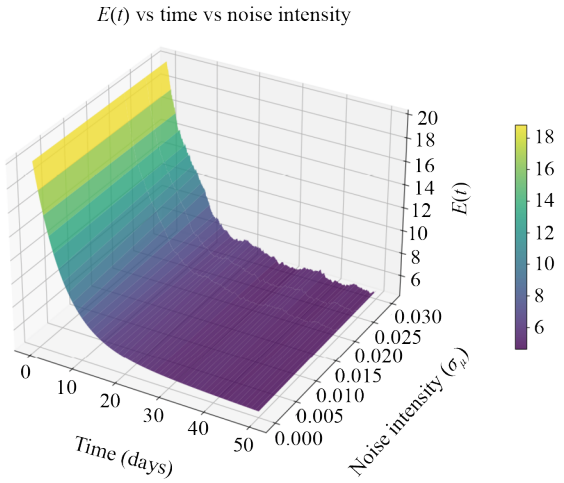

Figure 7. Surface of $E(t)$ versus (t, η) (with $\eta := \eta_S = \eta_E = \eta_R = \eta_V$)

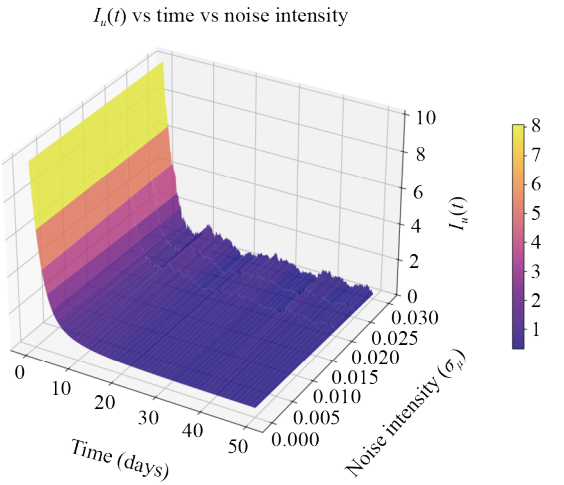

Figure 8. Surface of $I_u(t)$ versus (t, η)

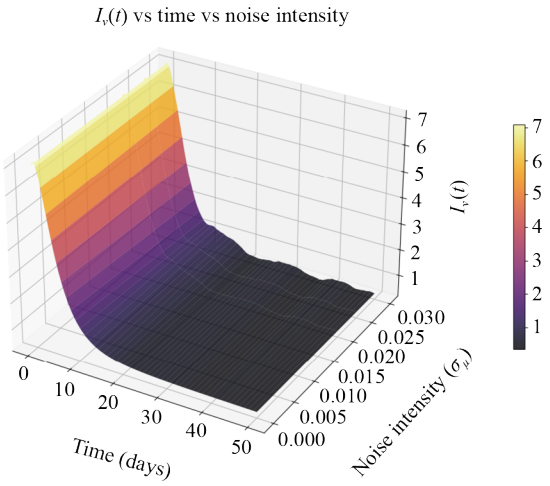

Figure 9. Surface of $I_v(t)$ versus (t, η)

Higher η broadens the envelope of (E, I_u) and, through the ln-Itô penalty, tends to depress I_v's effective growth while still permitting occasional stochastic surges. Together, these surfaces visualize how uncertainty redistributes burden in time and severity.

7. Discussion and conclusion

We developed and analyzed a stochastic SEIR-type model with two infectious classes, a primary class I_u (lower compliance) and a secondary class I_v (entered via a transition at rate σ), under saturated (Holling/Crowley-Martin) incidence. Environmental variability was modeled by multiplicative noises acting on mortality in selected compartments and on I_v; this preserves positivity and captures realistic random fluctuations.

Our analysis established a *noise-adjusted* reproduction quantity

$$R_s = R_0 - \frac{\eta_V^2}{2(\mu_2 + \gamma_v + \alpha_2)},$$

which provides a *sufficient* threshold: if $R_s < 1$ then the infection becomes extinct almost surely; if $R_s > 1$ then the infection is *persistent in the time-average sense*. This extends classical deterministic thresholds by showing how diffusion in an infectious class reduces effective growth via the negative Itô term in the logarithmic dynamics. Consequently, randomness can tip near-threshold systems toward extinction even when deterministic analysis predicts persistence.

Numerical experiments using a Milstein discretization consistent with the continuous model (saturated incidence; noise in S, E, R via W_1 and in I_v via W_2; no noise in I_u) illustrate these effects. As noise intensities increase, trajectories deviate from deterministic baselines, with earlier/later peaks, altered amplitudes, and higher extinction frequencies. Surface plots across noise levels visualize how uncertainty redistributes epidemic burden over time and severity, and scatter plots of final states show the dispersion of long-run outcomes.

7.1 *Implications*

Deterministic analyses may underestimate elimination prospects when systems are close to the threshold. Incorporating stochasticity yields risk-aware assessments for control planning (e.g., the likelihood of fade-out vs. resurgence) and helps interpret variability in observed epidemic waves.

7.2 *Limitations and extensions*

First, R_s here is a *sufficient* condition rather than the exact stochastic threshold (the latter corresponds to the top Lyapunov exponent of the linearized infection subsystem). Second, homogeneous mixing was assumed.

7.3 *Potential extensions*

The present framework can be extended in several meaningful directions. First, one may consider correlated or non-Gaussian noise (e.g., Lévy jumps or colored noise) to capture abrupt environmental shocks or seasonality. Second, incorporating time delays or spatial diffusion could reveal how latency and population mobility affect stochastic persistence and extinction. Third, hybrid approaches combining large-deviation theory with control optimization may help design cost-effective interventions that minimize the probability of epidemic resurgence. Finally, coupling the stochastic SEIR system with real epidemiological data could enable parameter inference and uncertainty quantification for practical forecasting.

7.4 *Conclusion*

Environmental noise materially shapes epidemic outcomes. The noise-adjusted threshold and consistent simulations together provide a practical lens for distinguishing extinction from persistence and for designing robust control strategies under uncertainty.

Availability of data and materials

No new data were generated or analyzed in this study.

Authors' contributions

All authors contributed equally to model formulation, analysis, simulations, and writing.

Acknowledgement

This research was funded by the Deanship of Scientific Research, Vice Presidency for Graduate Studies and Scientific Research, King Faisal University, Saudi Arabia [Grant No. KFU253854].

Conflict of interest

The authors declare no competing interests.

References

[1] Caraballo T, Settati A, Lahrouz A, Boutouil S, Harchaoui B. On the stochastic threshold of the COVID-19 epidemic model incorporating jump perturbations. *Chaos, Solitons & Fractals*. 2024; 180: 114521. Available from: https://doi.org/10.1016/j.chaos.2024.114521.

[2] Yang A, Song B, Yuan S. Noise-induced transitions in a non-smooth SIS epidemic model with media alert. *Mathematical Biosciences and Engineering*. 2021; 18(1): 745-763. Available from: https://doi.org/10.3934/mbe.2021040.

[3] McDermott A. Herd immunity is an important—and often misunderstood—public health phenomenon. *Proceedings of the National Academy of Sciences*. 2021; 118(21): e2107692118. Available from: https://doi.org/10.1073/pnas.2107692118.

[4] Chhetri B, Kumar BV. Stochastic mathematical modelling study for understanding the extinction, persistence and control of SARS-CoV-2 virus at the within-host level. *arXiv:2405.06403*. 2024. Available from: https://doi.org/10.48550/arXiv.2405.06403.

[5] Venkatesh A, Raj MP, Baranidharan B, Rahmani MKI, Tasneem KT, Khan M, et al. Analyzing steady-state equilibria and bifurcations in a time-delayed SIR epidemic model featuring Crowley-Martin incidence and Holling type II treatment rates. *Heliyon*. 2024; 10(21): e39520. Available from: https://doi.org/10.1016/j.heliyon.2024.e39520.

[6] Mahato P, Mahato SK, Das S. A stochastic epidemic model with Crowley-Martin incidence rate and Holling type III treatment. *Decision Analytics Journal*. 2024; 10: 100391. Available from: https://doi.org/10.1016/j.dajour.2023.100391.

[7] Hu X, Wang M, Dai X, Yu Y, Xiao A. A positivity preserving Milstein-type method for stochastic differential equations with positive solutions. *Journal of Computational and Applied Mathematics*. 2024; 449: 115963. Available from: https://doi.org/10.1016/j.cam.2024.115963.

[8] Mohammad KM, Kamrujjaman M. Stochastic differential equations to model influenza transmission with continuous and discrete-time Markov chains. *Alexandria Engineering Journal*. 2025; 110: 329-345. Available from: https://doi.org/10.1016/j.aej.2024.10.012.

[9] Lamperti J. Criteria for the recurrence or transience of stochastic process. I. *Journal of Mathematical Analysis and Applications*. 1960; 1(3-4): 314-330. Available from: https://doi.org/10.1016/0022-247X(60)90005-6.

[10] Wu X, Yan Y. Milstein scheme for a stochastic semilinear subdiffusion equation driven by fractionally integrated multiplicative noise. *Fractal and Fractional*. 2025; 9(5): 314. Available from: https://doi.org/10.3390/fractalfract9050314.

[11] Sabbar Y. A review of modern stochastic modeling: SDE/SPDE numerics, data-driven identification, and generative methods with applications in biology and epidemiology. *arXiv:2508.11004*. 2025. Available from: https://doi.org/10.48550/arXiv.2508.11004.

[12] Girardi P, Gaetan C. An SEIR model with time-varying coefficients for analyzing the SARS-CoV-2 epidemic. *Risk Analysis*. 2023; 43(1): 144-155. Available from: https://doi.org/10.1111/risa.13858.

[13] Ogunmiloro OM, Kareem H. Mathematical analysis of a generalized epidemic model with nonlinear incidence function. *Beni-Suef University Journal of Basic and Applied Sciences*. 2021; 10(1): 15. Available from: https://doi.org/10.1186/s43088-021-00097-9.

[14] Hussain S, Tunç O, Ur Rahman G, Khan H, Nadia E. Mathematical analysis of stochastic epidemic model of MERS-corona & application of ergodic theory. *Mathematics and Computers in Simulation*. 2023; 207: 130-150. Available from: https://doi.org/10.1016/j.matcom.2022.12.023.

[15] Mao X. *Stochastic Differential Equations and Applications*. Elsevier; 2007.

[16] Shah Hussain NI, Madi EN, Bakouri M, Khan I, Koh WS. On the stochastic modeling and forecasting of the SVIR epidemic dynamic model under environmental white noise. *AIMS Mathematics*. 2025; 10(2): 3983-3999. Available from: https://doi.org/10.3934/math.2025186.

[17] Gamerman D, Lopes HF. *Markov Chain Monte Carlo: Stochastic Simulation for Bayesian Inference*. Chapman and Hall/CRC; 2006.

[18] Ur Rahman G, Tymoshenko O, Di Nunno G. Insights on stochastic dynamics for transmission of monkeypox: Biological and probabilistic behavior. *Mathematical Methods in the Applied Sciences*. 2025; 48(15): 14316-14333. Available from: https://doi.org/10.1002/mma.11180.

[19] Wang L, Teng Z, Rifhat R, Wang K. Modelling of a drug resistant tuberculosis for the contribution of resistance and relapse in Xinjiang, China. *Discrete & Continuous Dynamical Systems-Series B*. 2023; 28(7): 4167-4189. Available from: https://doi.org/10.3934/dcdsb.2023003.

[20] Gasteratos I. *Moderate deviations for multiscale stochastic reaction-diffusion equations and related importance sampling schemes*. PhD Thesis. Boston, Massachusetts, United States: Boston University; 2022.

[21] Khasminskii R. *Stochastic Stability of Differential Equations*. Springer; 2012.

[22] Thakur T. *Stochastic Calculus and Brownian Motion*. Educohack Press; 2025.

[23] Higham DJ. An algorithmic introduction to numerical simulation of stochastic differential equations. *SIAM Review*. 2001; 43(3): 525-546. Available from: https://doi.org/10.1137/S0036144500378302.